Food Control 137 (2022) 108943

Contents lists available at ScienceDirect

Food Control

journal homepage: www.elsevier.com/locate/foodcont

Fast DNA biosensing based on isothermal amplification, unmodified gold nanoparticles, and smartphone detection

Luis A. Tortajada-Genaro [a,b,*], María Isabel Lucío [a], Ángel Maquieira [a,b]

[a] Instituto Interuniversitario de Investigación de Reconocimiento Molecular y Desarrollo Tecnológico (IDM), Universitat Politècnica de València, Universitat de València, Camino de Vera s/n, 46022, Valencia, Spain
[b] Dep. Química, Universitat Politècnica de València, Camino de Vera s/n, 46022, Valencia, Spain

ARTICLE INFO

Keywords:
Naked-eye detection
Unmodified nanogold
Isothermal amplification
Smartphone biosensing
Gluten

ABSTRACT

The protection of the consumer against foodborne illnesses and fraudulent practices requires methods capable of detecting critical components. Classical instrumental and DNA-based technologies have assay time, portability, and cost limitations. Thus, food control needs alternative methodologies for massive and cost-effective screening. Herein, we report an instrument-free method based on detecting genes that encode proteins related to food allergies and ingredients associated with illegal practices. Tailed recombinase polymerase amplification (tailed-RPA) provided the selective isothermal amplification of target regions. A reproducible and fast optical detection was developed based on the salt-induced aggregation of 15 nm gold nanoparticles (AuNPs). The target presence was directly observed (naked-eye detection) and quantified using a smartphone and RGB image decomposition. The advantages arise from the effective formation of a hybrid complex between non-functionalized nanoparticles and amplification products with a single-strand tail, featuring short incubation time, simplicity, and low sample and reagent volumes. As proof of concept, two targets were determined: *trnL* gene and ITS region. The first sequence is located in the chloroplast genome of cereals and is valuable to control the adulteration of meat products. The second is a fragment common to the three main gluten-containing cereals, applicable to the indirect detection of this allergen. The novelty also is the integration of a low-cost assay platform and a straightforward interpretation system to foster its implementation in the industry. The RPA-AuNP assay offered a good sensitivity (genomic DNA 0.8 ng), selectivity (absence of unspecific response), reproducibility (standard deviation 2–11%), and accuracy in marketed food products (100%). Therefore, a competitive biosensing system enables better control according to food industry/consumers demands from Farm to Fork strategy.

1. Introduction

Prevention and control systems are required throughout the food chain by checking every segment from production to the consumer. The application of biomolecular techniques in laboratories, such as immunoassays and DNA-based techniques, increases every day (Bansal et al., 2017; Lo & Shaw, 2018). They provide valuable information to determine compliance with voluntary thresholds (industrial practices) or mandatory requirements (law and regulations). PCR-based methods lead the bioanalytical techniques due to extraordinary sensitivity and specificity. But, most are not affordable enough, user-friendly, rapid considering the requirements of massive use in the food sector. For instance, an essential drawback of PCR-based methods is the requirement of lab-based thermal cycler and detection equipment (e.g., gel electrophoresis, fluorimeter). Additionally, more than 90% of the total time is due to temperature cycling rather than amplification. In the last decades, advances have provided new tools for fast, portable approaches. The proposed solutions include portable thermal cyclers, qPCR instruments, microfluidic devices based on isothermal amplification techniques, and nanomaterials for non-fluorescent detection.

Gold nanoparticles (AuNPs) are excellent optical transductors enabling a viable alternative for colorimetric sensing (Valentini & Pompa, 2013). These nanomaterials show a strong light absorption within the visible region due to localized surface plasmon resonance. Their color is tunable depending on the particle size, and their aggregation causes a visual color change.

* Corresponding author. Instituto Interuniversitario de Investigación de Reconocimiento Molecular y Desarrollo Tecnológico (IDM), Universitat Politècnica de València, Universitat de València, Camino de Vera s/n, 46022, Valencia, Spain.
E-mail address: luitorge@qim.upv.es (L.A. Tortajada-Genaro).

https://doi.org/10.1016/j.foodcont.2022.108943
Received 7 January 2022; Received in revised form 23 February 2022; Accepted 2 March 2022
Available online 4 March 2022

Several colorimetric methods have exploited the aggregation of AuNPs upon selective recognition of target nucleic acids or other analytes (Chang et al., 2019). An interesting review article about the application in detecting food nuisances has been recently published, including heavy metals, veterinary drug residues, pesticide drug residues, toxins, and hazardous substances (Chen et al., 2018). In the most general category of AuNPs-based assays, the target nucleic acid acts as a cross-linker between two DNA-functionalized particles, complementary to two adjacent regions on the target sequence (Cao et al., 2002). However, they require precise covalent modification and a long preparation time.

Alternatively, direct salt-induced aggregation of unmodified nanoparticles has been used (Li & Rothberg, 2004). The repulsion of initially adsorbed negative ions (e.g., citrate) at high salt concentrations is screened. Thus, the strong van der Waals attraction between AuNPs leads to a color change compared to colloidal gold. The biosensing principle resides on the stabilization caused by several molecules. As the presence of single-strand DNA (ssDNA) inhibits this process, screening assays have been reported based on unmodified gold particles (Li et al., 2018; Yun et al., 2016). However, the described naked-eye solutions have been demonstrated for ssDNA targets at high concentrations (nM-μM) or PCR products after a denaturing process, reducing the potential features of this biosensing assay.

Recent studies reported a gold nanoparticle-mediated method combined with loop-mediated isothermal amplification (LAMP) for the rapid and accurate diagnosis of pathogens (Srimongkol et al., 2020; Ye et al., 2018).

Isothermal amplification reactions simplify the process by avoiding the thermal aperture of the double-stranded template at 90–95 °C. Specific primer designs, polymerases, or combinations of enzymes achieve replication as an alternative to the conventional approach (Li & Macdonald, 2015; Zhao et al., 2015). Then, reactions are performed using only a heating block, peltier, ovens, or similar heating systems. Applications of the consequent simplified and miniaturized assays have demonstrated sensitive detection of target genes with rapid-response, cost-effectiveness, high robustness, and reproducibility (Giuffrida & Spoto, 2017). Different technologies have been coupled to isothermal techniques for the sensitive detection or quantification of amplified products, such as electrochemistry, microarrays, and dye-based fluorometry (Deng & Gao, 2015). But, in some cases, the proposed solutions are not instrument-free or require specific chips, limiting the actual implementation to decentralized laboratories.

Our research aimed to develop a colorimetric AuNPs-mediated method for the enhanced detection of genes that encode proteins related to food safety. The adsorption mechanism is based on electrostatic interaction, then the functionalization of particles or the target DNA is not required. The research focused on a novel integration of an isothermal amplification technique and smartphone detection. The chosen isothermal technique is recombinase polymerase amplification (RPA) using tailed primers. Compared to other isothermal processes, this reaction shows essential advantages, such as low working temperature (36–40 °C), simple primer design, fast-amplification (20–60 min), no initial heating step, and robust to biological substances (Lobato & O'Sullivan, 2018). In addition, this amplification is compatible with several assay formats for point-of-need applications (Santiago-Felipe et al., 2016; Tortajada-Genaro et al., 2019). The goal was to generate RPA products with single-strand regions to modify the color of gold colloidal suspension, which can be detected with the naked eye even at a relatively low concentration.

Furthermore, an assay of RPA-AuNPs, supported on smartphone detection, provided an objective interpretation to be potentially applied in several food safety scenarios. Therefore, the novelty of this research is the colorimetric detection of products from an isothermal amplification technique based on the aggregation of unmodified AuNPs and its reliable read-out. Without oligo functionalization, thermal cycles, probe hybridization, or fluorescence labeling, the studied approach adds more simplicity and portability to the DNA-based screening of food products.

2. Material and methods

2.1. Reagents and materials

Nucleotide sequences of target genes were obtained from the National Biotechnology Information Center database (NCBI) (https://www.ncbi.nlm.nih.gov/) and satisfactorily confirmed by the NCBI's Basic Local Alignment Search Tool (BLAST) (https://blast.ncbi.nlm.nih.gov/Blast.cgi). The sequences of the specific primers designed are shown in Table SI1. All the oligonucleotides, purified by HPLC, were purchased from Eurofins Genomics (Germany).

AuNPs were prepared according to literature (González-Domínguez et al., 2018). Briefly, a trisodium citrate dihydrate solution (12.5 mL, 38.8 mM) was added to a boiling solution of gold (III) chloride trihydrate (250 mL, 0.5 mM) for reagents from Sigma-Aldrich. The resulting mixture was stirred for 15 min until a wine-red color was obtained and, subsequently, cooled at room temperature at low stirring. The prepared AuNPs were characterized by transmission electron microscopy and UV–Visible spectroscopy. Particles were concentrated by centrifugation at 10,000 rpm for 10 min (2 cycles) and kept at 4 °C. The final concentration was adjusted to 4 nM.

2.2. Samples and DNA extraction

For optimization and in-house experimental validation, binary mixtures of pure ingredients -wheat flour and onion - were prepared. For optimizing the application of cereal detection, mixtures of flours and minced meat from chicken (0–20%) were prepared. For the application of gluten detection, gluten-free ingredients and wheat flour at representative low spiked levels. The gluten amount was established, assuming the percentage of gluten proteins as an overall 10% of the cereal weight (Biesiekierski, 2017). The novel RPA-AuNP method and reference methods analyzed commercial products bought in local supermarkets.

Genomic DNA of food products was extracted using spin column technology (GMO Extraction Kit, Life technologies). The concentration (ng/mL) was determined by spectrophotometry (NanoDrop 2000c; ThermoFisher Sci.) and by fluorimetry (Qubit dsDNA HS Assay Kit, ThermoFisher Sci.). Solutions of the purified genomic DNA were diluted to 4 ng/μL.

2.3. Tailed-RPA amplification and colorimetric detection

The reagents used for the genomic DNA amplification came in the TwistAmp Basic RPA kit (TwistDx, UK). The mixtures (10 μL) were prepared with the enzyme pellet in rehydrated buffer, 7 mM of magnesium acetate, 240 nM of upstream primer (tailed primer), 240 nM of downstream primer, and 4 μL of DNA extract. Each experimental batch included a negative sample (human genomic DNA) as an assay control. The employed heating system was a thermal block, operating at 37 °C for 40 min. RPA products were purified by a silica column (PCR purification kit, Jena Bioscience, Germany), following the manufacturer's instructions.

The products (1 μL) were mixed with the detection solution (5 μL), containing AuNPs at 1:10 dilution and citrate buffer at 100 mM pH = 6.75, and dispensed onto a plastic membrane (Parafilm®, Bemis Company, Inc.). The addition of NaCl solution at 100 mM (4 μL) started the aggregation. After 10 min, the observed color was registered, and a smartphone (Huawei P10 Plus) captured images of the solution drops under controlled illumination conditions (Figure SI1). Image analysis was performed by two free-access software. Color Detector RGB (application for Android) allowed direct processing in the smartphone, and the ImageJ software (National Institutes of Health, USA) processed the images on a personal computer. For the quantitative determination,

the output was the red channel signal minus the signal of the blue channel (R–B).

2.4. Reference methods

Electrophoresis detection. The amplification products were determined by electrophoretic separation in 3% (w/v) agarose gels at 110 V potential for 30 min. The samples were mixed with loading buffer (glycerol loading dye, Fisher Sci.) and fluorescent dye (Real Safe staining, Durviz, Spain) and loaded on the gel. Bands were visualized using a transilluminator at 312 nm (ECX-F20.M, Vilber, Germany), and the product length was determined using a size standard (mini DNA ladder 50 bp ExactGene, Fisher Sci.).

Real-RPA. Real-time thermocycler (TS2, Qiagen) was also used to optimize the RPA assay in real-time and end-point formats.

PCR. The reaction mixture (12.5 μL) was prepared by adding 0.4 U Taq polymerase, 3 mM $MgCl_2$, and 200 μM dNTPs to the reaction buffer. The primer concentrations used for asymmetric amplification were 0.1 μM/0.4 μM (forward/reverse), and the amount of DNA template was 4 ng of food samples. Each experimental batch included a negative sample (human genomic DNA) as an assay control. The thermocycling was carried out in a TC400 thermocycler (Bibby Scientific, UK) as follows: 95 °C for 5 min for initial activation; 40 cycles of denaturing at 94 °C for 30 s, annealing at 57 °C for 30 s, and extension at 72 °C for 30 s; and 72 °C for 5 min for a final extension. The amplification factor was calculated from the synthesized copies and the initial amount of genomic DNA.

qPCR. The amplification was carried out in 96-well microplates (Axygen PCR, Fischer Scientific), containing 1x TB Green Premix Ex Taq (Takara), 1x ROX reference dye II (Takara), 300 nM of each primer, and 1 μL of each DNA extract (4 ng/μL, equivalent to 1300 copies). The instrument was ViiA 7 Real-Time PCR System (Applied Biosystem, USA). The thermal cycling was: 2 min at 50 °C, 10 min at 95 °C, followed by 35 cycles of amplification of 1 s at 95 °C (denaturation), and 35 s at 60 °C (primer annealing and extension, fluorescence acquisition). Reactions were run in duplicate, and the experiment included one negative control and no template control. Optionally, a melting curve analysis was acquired from 60 °C to 95 °C at a thermal transition rate of 0.5 °C per second.

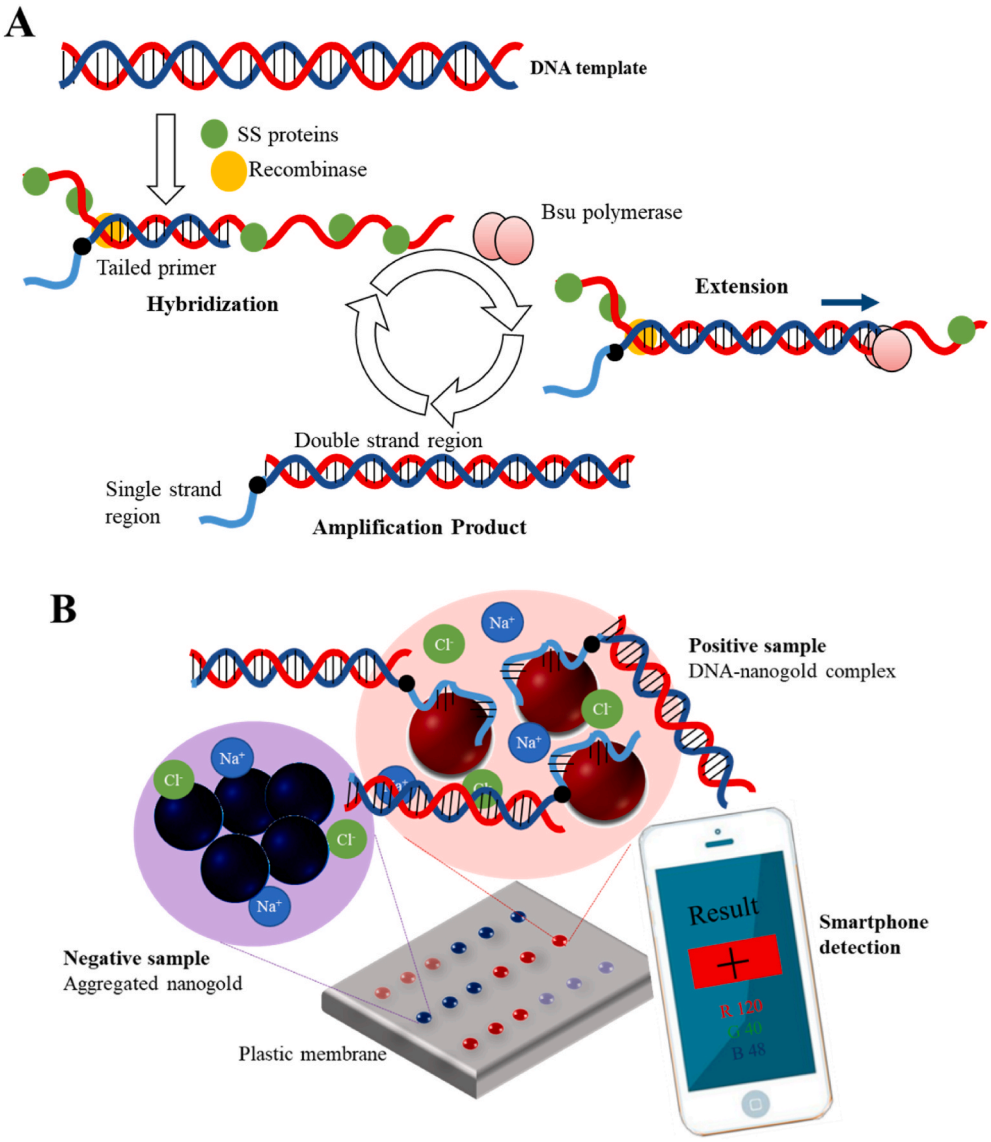

Fig. 1. Assay principle: (a) isothermal amplification reaction using tailed primers and (b) read-out based on a salt-induced aggregation of unmodified gold nanoparticles, performed in a drop format on a plastic membrane, and smartphone imaging.

3. Results and discussion

3.1. Method principle

The assay consisted of the specific amplification of target sequences under isothermal conditions using tailed primers (tailed-RPA) and the incubation of generated products with the gold nanoparticles in the presence of sodium chloride at high concentrations (Fig. 1).

Where the DNA target is not present, the amplification is not produced, and nanoparticles aggregate, observing the decrease of surface plasmon resonance band at low wavelengths and the increase of the band at high wavelengths. Meanwhile, the presence of target genes generates tailed-RPA products, inducing their adsorption onto AuNP based on van der Waals forces. The formation of complexes (ssDNA-AuNPs) produces superficial negative charges. Hence, the stronger electrostatic repulsion stabilized against salt-induced aggregation, keeping the optical properties of the colloidal state. The target presence can be directly observed (naked-eye detection) and accurately quantified using a smartphone camera and color channel decomposition.

3.2. Study of detection conditions

The experimental variables that control the aggregation of unmodified nanoparticles and smartphone detection were examined. The features of the synthesized AuNP solution were characterized (Figure SI2). From transmission electron microscopy data, the diameter of the AuNPs was 14.9 ± 2.6 nm. UV/Vis spectroscopy data showed that the absorption band centered at 530 nm indicated a correct synthesis, and the number density of particles was $1.18{\cdot}10^{11}$ (Table SI2).

The following experiments verified robust, sensitive, colorimetric-based biosensing. As expected in the absence of DNA, the color of the AuNP solution changed from ruby-red (colloid state) to purple-gray (aggregated state) after the addition of NaCl (Fig. 2a). The registered spectra changed, increasing the concentration of salt. The absorption

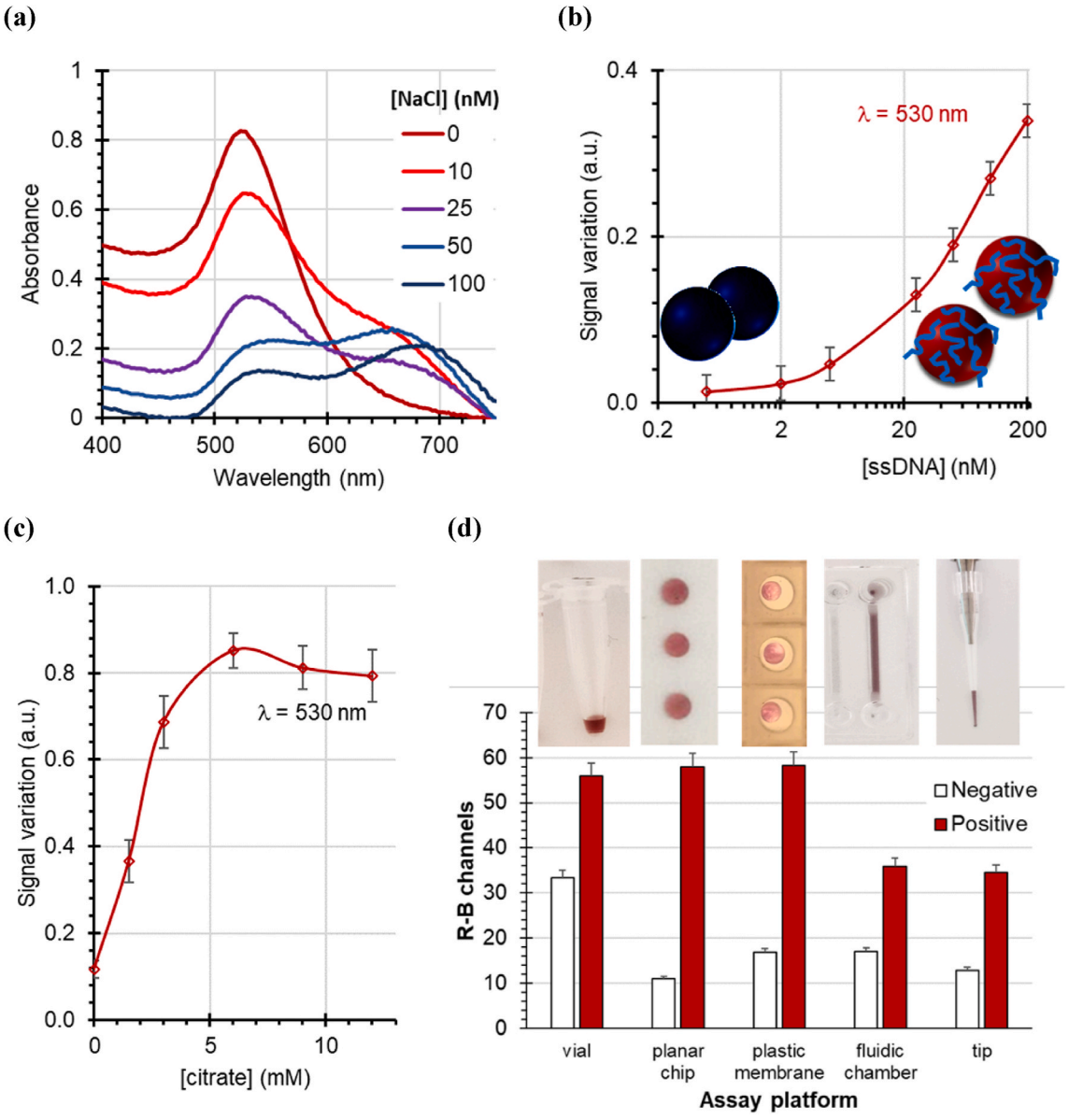

Fig. 2. Formation of hybrids between DNA and 15 nm-nanogold particles: (a) Effect of sodium chloride concentration. (b) Effect of ssDNA concentration on the optical signal variation (absorbance difference between ssDNA solution and blank). Insert: scheme of ssDNA-grafted AuNPs. (c) Effect of citrate concentration on the optical signal variation (absorbance difference between ssDNA solution and blank). (d) Platform selection considering signal from red (R) and blue (B) channels. Studied ssDNA: TCTATGCGACAGGCAGTACCGTAACCATTT CCGCA GCCGCAA (42 nucleotides).

band at 530 nm decreased, whereas the adsorption band at 650 nm increased. Hence, this variation of optical properties confirmed the salt-induced aggregation.

The process was also performed in the presence of ssDNA, using a sequence of 42 nucleotides for checking experimental feasibility. According to the measured diameter of 15 nm-AuNPs, the active surface is approximately 700 nm^2. Thus, the estimated surface coverage was 16 DNA molecules per one AuNP, considering a disorderly layer of rod-like molecules in a stretched conformation (Table SI2). The experiments performed revealed several facts (Fig. 2b and c). (i) The aggregation process was reduced or avoided based on the spectrophotometric data, keeping the maximum surface plasmon resonance band at 530 nm. (ii) Citrate buffer improved the recognition process. (iii) The method was sensitive to the DNA content, producing positive responses up to 1 nM. Since the solution volume was 1 μL, the ssDNA amount was 1 fmol.

The next goal was to explore the analytical capabilities of the smartphone for imaging the hybrids between AuNP and nucleic acids. Several authors have pointed out that the use of mobile phones as detection systems of colorimetric biorecognition events is not as easy as expected (Yu & Wei, 2018). Although the smartphone integrates a high-sensitive camera, reproducible biosensing required measurements obtained only under specific experimental conditions. As previously described (Yamanaka et al., 2018), the distance and illumination were critical for the image quality of bioanalytical platforms. The present study confirmed that photos taken under non-controlled illumination conditions were invalid. Some approaches, such as the flashlight of a smartphone camera or external vertical light sources, produced irregular reflections or poor image quality. In contrast, the reading chamber with holes for diffuse light provided excellent reproducible images without the need for a light source, and it maximized the differences between ssDNA standards (colloidal AuNP, red) and blanks (AuNP aggregation, purple) (Figure SI1).

Regarding image processing, the RGB analysis of assay drops delivered reliable results. The comparison of all possible data processing depicted that the best results, in terms of sensitivity and reproducibility, were obtained for R–B values. The blue channel signal, mainly associated with aggregated nanoparticles, was subtracted to the red channel signal, mainly associated with colloid gold nanoparticles (Table SI3). The result was a high signal-to-noise ratio (>25) and a low standard deviation between replicates (relative standard deviation 4–8%), and a significant signal variation that discriminated solutions with different concentrations of DNA.

Experiments were conducted to compare values obtained from different smartphone manufacturers. Due to their camera-specific features and image processing algorithms, differences in quality images were observed. Sophisticated calibration procedures can homogenize the read-out, but they are challenging to implement in most sensing scenarios (Kanchi et al., 2018). Some recommendations can be proposed for a robust response independently on the used phone, minimizing the image processing. Good results were obtained using constant illumination, a high number of pixels per drop, and R–B values as the output signal rather than a single channel value. Another solution is using color patterns to correct experimental variations (Yamanaka et al., 2018).

A disposable sensing platform requires low-cost and easy-to-use consumables intended for short-term or rapid single-point measurements and easy-handling of reagents and samples (Dincer et al., 2019). Several platforms for performing bioanalytical assays were compared in parallelized experiments (Fig. 2d). They included conical tubes (Li et al., 2018; Ye et al., 2018; Yun et al., 2016), planar chip (Tortajada-Genaro et al., 2019), plastic membranes (Kim et al., 2018; Yu & Shi, 2015), fluidic chips (Santiago-Felipe et al., 2016; Yang et al., 2016) and pipette tips (Sharafeldin et al., 2019). Concerning the camera-based read-out, some platforms showed high responses for controls due to the reflectivity of raw materials and their conical shape. Plastic membranes, consisting mainly of paraffin wax, provided a high and reproducible signal-to-noise ratio of drops and a higher signal difference between ssDNA standards and blanks. In addition to the good optical performances, the platform had a lower price and was highly resistant to many chemical substances. Even though this plastic is used extensively in laboratories as sealing material, as previous studies and current experiments demonstrated, it also has excellent features as biosensing support of AuNP solutions.

3.3. Optimization of RPA conditions

The isothermal amplification was developed following the requirements for a fast assay (Santiago-Felipe et al., 2016). Thus, short target region (<200 bp) and short primers (18–20 nucleotides) were selected. Regarding the reaction conditions, a 40-min incubation at 37 °C achieved signal saturation applied to genomic DNA from positive and negative samples (Fig. 3a). Fluorescence measurements indicated sensitive and precise amplification yields ($>10^7$). However, the direct detection of RPA products, based on the AuNPs method, led to erroneous results. Experiments confirmed that several components of the RPA reaction, such as salts, DNA binding proteins, or detergents, interfered in the latter aggregation of nanoparticles (Fig. 3b). A silica-column purification step to isolate RPA products from reaction reagents or ions in food samples avoided unspecific AuNP aggregation.

The developed sensing method was applied to detect the amplification products from food mixtures. Smartphone registered clear images of drops, and differential RGB profiles were obtained depending on the absence or presence of RPA products (Fig. 3c). Compared to other end-point strategies described for isothermal techniques (Lobato & O'Sullivan, 2018), the correct integration of the RPA-AuNP assay is a versatile naked-eye solution and enhanced by smartphone read-out. Thus, these experiments confirmed its potential use as a colorimetric biosensing method of target DNA genes.

A paired experiment compared the amplification features of the novel isothermal mode (RPA) and an approach based on thermal cycling regime (PCR) (Zou et al., 2018). Statistics analyses confirmed that both amplification methods provided comparable mean signals (*t*-test, $t = 2.53$, p-value > 0.05) and comparable standard deviations (F-test, $F = 0.73$, p-value > 0.05). Therefore, the method excluded the requirement of heavy thermocyclers, evidencing that the assay can be done at field sites.

The improvement of the assay sensitivity was investigated, considering the use of tailed primers. The central idea was to take advantage of the electrostatic properties of single-strand DNA compared to double-strand DNA (Chang et al., 2019; Chen et al., 2018; Valentini and Pompa, 2016). The proposed RPA-AuNP assay was applied to reaction mixtures containing conventional or tailed forward primers (Fig. 4). The tailed primer was composed of a non-complementary sequence (5′-end) and specific-gene sequence (3′-end) separated by C3 spacer. So, this short carbon chain prevented the extension of copied strand during the isothermal amplification beyond the complementary sequence. Thus, the 5′-end tail was in a single-strand configuration during all amplification cycles. In a primer without the C3 spacer, the polymerase can extend the template copy until the 5′-end, losing the original proposal. Besides, the tail must show a null complementary to either genome to avoid cross-reactivity.

Although the amplification yield decreased (approx. 38%), the final response measured by the smartphone increased (approx. 22%). These results confirmed that the charged phosphate backbone of the double-strand amplification product competed with the adsorbed citrate ions reducing the electrostatic interaction on the nanogold surface. But, the presence of a single-strand tail in RPA products favored the formation of complexes because its structure permitted the uncoiling needed to expose the bases. The interaction between the DNA bases and the AuNPs was sufficient to cause RPA products to stick to the surface, inhibiting the aggregation of nanoparticles.

The RPA-AuNP method overcame the methods that require thermal opening of products or amplification techniques in asymmetric format

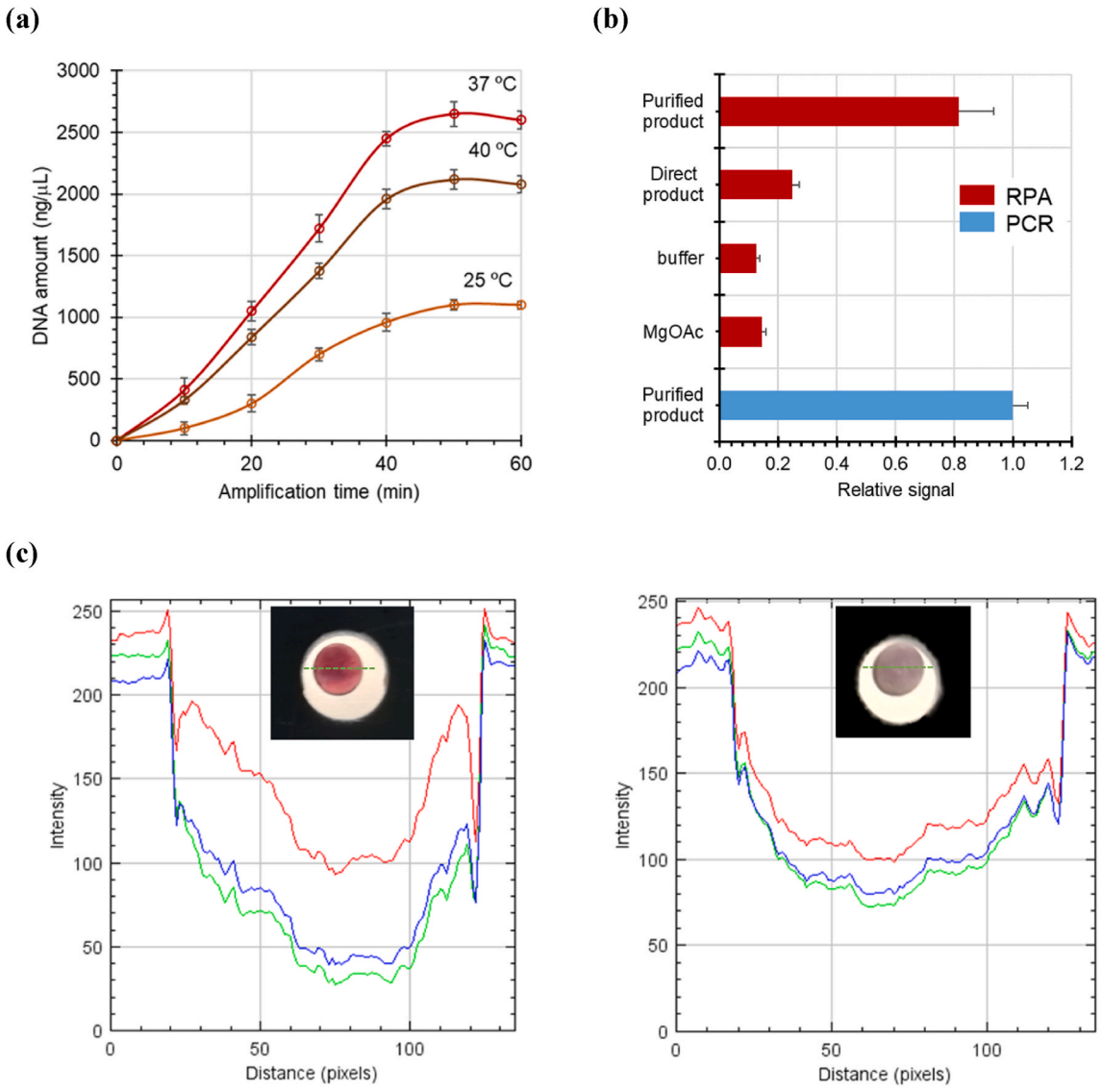

Fig. 3. Optimization of isothermal amplification based on RPA reaction. (a) Amplification kinetics. (b) Inhibition of RPA components on the aggregation of nanogold particles. The graph represents the measured response of the RPA-based method or RPA components compared to the PCR-based method. (c) RGB profile and image of a drop for a negative sample (left) and a positive sample (right). The graph represents the optical intensity of each channel vs. distance in a secant line over the drop. DNA template: 4 ng from pure wheat flour. Amplification target: trnL gene. *** *t*-test: p-value < 0.001.

(Li et al., 2018; Yun et al., 2016). The consequence was a high amplification yield using a simpler heating system for keeping the temperature constant. In conclusion, the assay was demonstrated using materials available in low-resource laboratories, such as a small centrifuge, a heat block, an expanded polystyrene box, a lamp, and a smartphone. Thus, the method excluded the requirement of heavy thermocyclers, fluorescence readers, or other instruments. For assays performed at the field site, some technologies can used, such a Peltier cooler/heater and a flashlight. Equipment is low-cost and can be transported in a mobile suitcase laboratory and battery-powered, competitive solution compared to current portable RT-PCR instruments. Also, there are solutions to convert it into an instrument-free assay, such as magnetic DNA extraction, exothermic heating, and naked-eye detection (Lobato & O'Sullivan, 2018).

3.4. Detection of food adulteration

Considering achieved performances, a compatible application was detecting adulterants in foods (Bansal et al., 2017). The processing of certain meat products can include the addition of cereals to improve their functional properties, such as water- and fat-binding, texturizing properties, low cost, and supplementation of dietary fiber-rich vegetative. Thus, it is helpful to determine whether the added amount is lower than a regulated threshold value. Then, we designed an RPA-AuNP assay to detect a cereal-specific gene (trnL gene) to monitor food quality (Table SI1). Firstly, an *in-silico* method selected short RPA primers without homology to other potential genes and avoided stable secondary structures. The following experiments checked the amplification specificity discriminating pure food ingredients. The images obtained from gel electrophoresis depicted a single amplification band at the expected position (Fig. 5a), so the amplification and post-amplification treatment were effective. Also, data from melting temperature analysis (Fig. 5b) and qPCR (Fig. 5c) confirmed the accurate amplification of the target sequence. Only unspecific products were detected using a high amount of non-target templates and high amplification cycles.

The incubation of RPA products with AuNPs/NaCl produced the expected behavior (Fig. 5d). Cereal-containing samples generated tailed RPA products that stabilized AuNPs against the aggregation, reporting

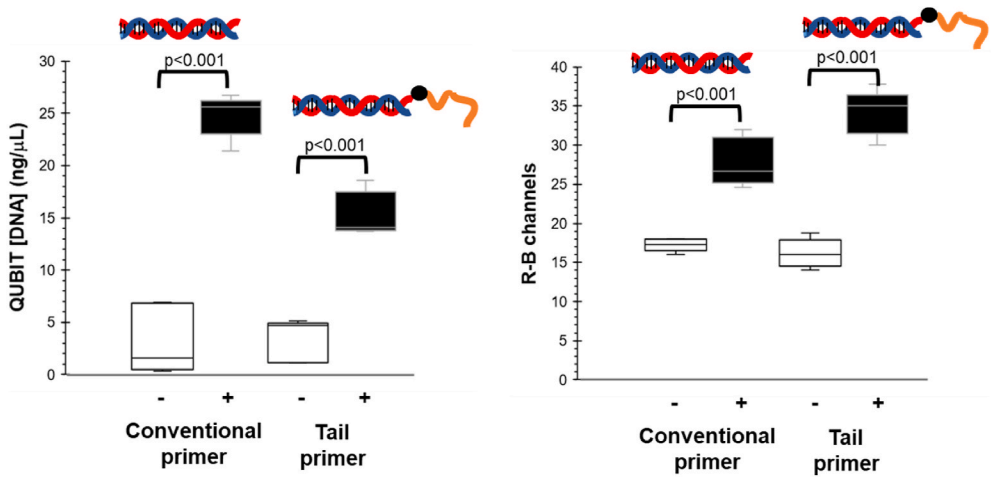

Fig. 4. Assays for signal improvement, comparing conventional and tail primers applied to negative samples (−) and positive samples (+). (a) Concentrations of RPA products measured by the fluorescence method (Qubit reagents and equipment). (b) Registered signal based on smartphone detection. *t*-test at 95% confidence percentage. The black dot indicates the C3 spacer between the gene-specific sequence and the 5′-tail sequence (orange line).

high signals for the Red channel and low for Green and Blue channels. In contrast, the analysis of non-target samples produced similar responses to negative controls, indicating the number of unspecific copies was insufficient to keep the colloidal state. Hence, the assay selectivity was achieved thanks to the RPA mechanism, being the replication of target templates highly efficient and the formation of non-specific products negligible. The novel instrument-free approach correctly identified cereals, demonstrating the absence of false-positive results. The detection limit was determined by diluting a DNA extract from a wheat sample. The lower concentration that provided a positive response was 0.2 ng/μL (0.8 ng). Considering the genome of wheat (17 Gb), the estimated detection limit was 11 copies/μL (44 copies).

The next challenge was the quantitative study of the response depending on the food composition. The assay sensitivity was established from prepared foods and compared to a conventional qPCR method (Fig. 6). The chromaticity of drops varied depending on the adulteration level of food products. The optical responses and the logarithm of adulteration percentage fitted by a linear function, with excellent correlation. Although qPCR achieved a better detection limit, the RPA-AuNPs method discriminated the adulterated samples containing the target ingredient up to 0.5%. Hence, the results demonstrated the reliability of our biosensing method applied to routine food control, considering the current practice.

3.5. Detection of gluten in marketed food products

The following challenge was the application for the indirect detection of food allergens; concretely, gluten due to its relevance and the need for fast, reliable methods. Our target region was a fragment common to the three main gluten-containing cereals (wheat, barley, and rye) and located in the ribosomal Internal Transcribed Spacer-2 region (ITS). This region has been described for accurately tracking gluten presence based on the selective discrimination of target genomes against other plant species (García-García et al., 2019).

After optimization experiments (Figure SI3) using specific ITS oligonucleotides (Table SI5), the analysis of food mixtures containing flour of target cereals estimated assay performances. The detection limit was the minimum concentration level that produced a distinguished signal from the non-target flour. The novel colorimetric method detected up to 0.5% wheat (225 mg gluten/kg). This detection limit was higher than those achieved by qPCR in this study and described in previous papers based on ELISA, qPCR, or qLAMP (Garrido-Maestu et al., 2018; Scherf & Poms, 2016). However, these results demonstrated the possibility of performing rapid DNA testing about gluten presence without requiring high-qualified personnel or expensive laboratory equipment such as thermocyclers or complex readers. The main advantages of RPA against LAMP approaches are the lower working temperature, more straightforward primer design, and lower probability of false-positive.

Under these conditions, the assay was sensitive and reproducible enough to analyze commercial food products. As shown, the observed color and the image analysis followed a clear pattern (Table 1). Accurate, reproducible discrimination between gluten and gluten-free foods was achieved in an easy-to-perform mode. A relevant limitation to field test was the DNA extraction step, considering time and the required equipment, i.e., centrifuge. Hence, a future improvement is magnetic beads-based extraction to overcome this bottleneck. After DNA extraction, the assay was rapid, and times were: 40 min for RPA, 10 min for purification, 10 min for AuNPs aggregation, and 5 min for imaging and image analysis.

4. Conclusions

Screening applications based on short-term or single-shot measurements in the food field demand disposable DNA biosensing systems. AuNPs-based detection methods provide engaging performances for versatile solutions, overcoming traditional limitations regarding assay time and portability of conventional techniques. The direct interaction with unfunctionalized nanoparticles, without oligo functionalization, adds more simplicity and reduces the testing cost. The success of the newly-developed method comes from the effective integration of the RPA technique, a versatile colorimetric transducer, and a universal reader such as a smartphone.

Compared to previous approaches, the novelty arises from the chosen isothermal amplification reaction and how ssDNA is produced for AuNP-mediated detection. First, RPA is easy-designed, fast, robust, and high tolerant for inhibitors. Secondly, RPA-methods operate at a constant low temperature, enabling the amplification without the need for typical PCR thermocyclers and expensive laboratory equipment. Third, tailed primers are a direct mode to generate single-strand products, avoiding partially ineffective post-amplification steps, such as enzymatic digestion or thermal denaturation. As far as we know, the developed method is the first colorimetric assay based on an isothermal amplification technique for gluten detection.

On the other hand, smartphones are increasingly applied for limited-resource settings allowing easy-to-operation DNA testing. As demonstrated, several experimental variables affect the system performances because they change the optical features captured on smartphone cameras. Therefore, this study contributes to establishing the feasible

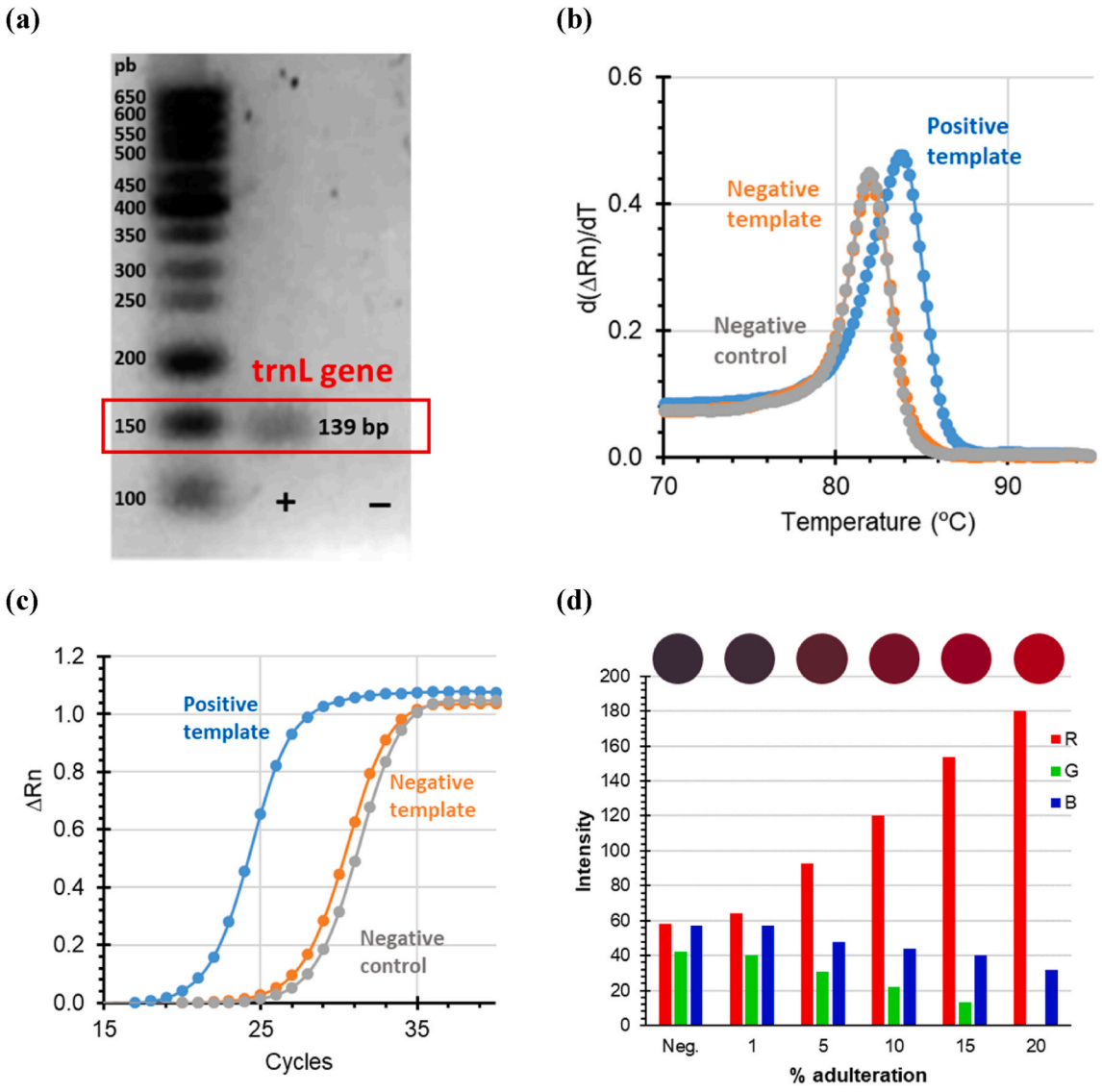

Fig. 5. Comparison of methods applied on the identification of cereals: (a) gel electrophoresis of purified RPA product, (b) melting temperature analysis, (c) qPCR, and (d) AuNPs/smartphone method. Negative control: amplification reagents. Negative template: non-target DNA. Agarose gel electrophoresis. Lane 1, mini DNA ladder (50 bp ExactGene, Fisher Scientific International Inc.). Lane 2, cereal sample. Lane 3, meat sample. qPCR method. ΔRn: net fluorescent signal from TB Green channel divided by the passive reference dye channel (Rox).

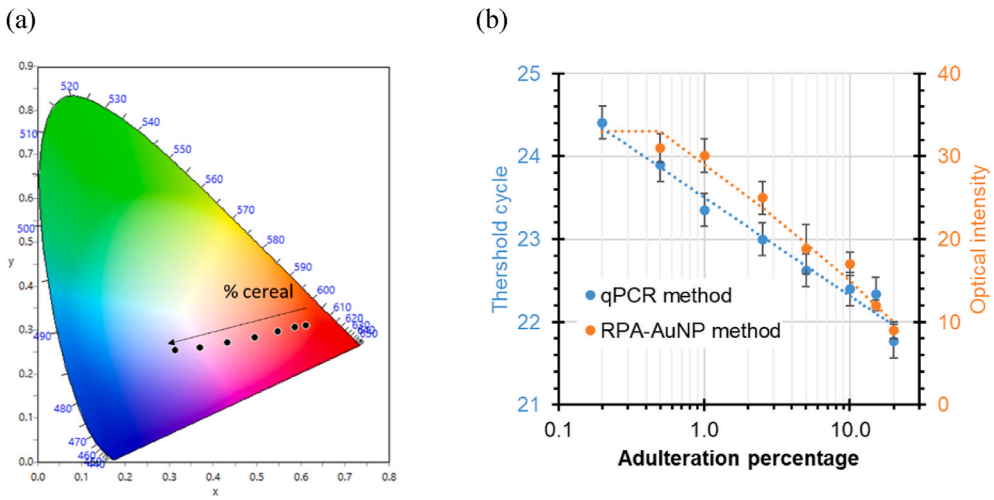

Fig. 6. Detection of cereal content in meat/flour mixtures: (a) Variation of chromaticity coordinates in CIE1931 plot, increasing the cereal percentage in meat product. Conversion of RGB coordinates to (x,y) coordinates was based on the tristimulus functions. (b) Comparison of method results for the AuNPs and qPCR methods. Samples: mixtures of wheat flour and minced chicken meat. Linear equations: $y = 23.5–1.2 \cdot x$, $R^2 = 0.98$ for qPCR method and $y = 28.9–13.2 \cdot x$, $R^2 = 0.96$ for RPA-AuNPs.

Table 1
Results obtained applying the developed method for the detection of the gluten-related gene. Replicates = 3..

Foods	Declared	Color	R-B channels	Detected
Noodles	+		86±10	+
Flour I	+		106±13	+
Baby food	+		77±9	+
Snacks I	+		76±9	+
Cookies	+		92±11	+
Flour II	-		19±2	-
Candy	-		16±2	-
Sausage	-		18±2	-
Processed meat	-		19±2	-
Snacks II	-		17±2	-

R-B values: mean±standard deviation

requirements to transform this consumer electronic device into an analytical reader of results generated.

Following the developed methodology, the assays are complete within 2 h, and the low amount of the target DNA (0.8 ng) produces color changes. A smartphone can directly measure them for quantifying the target ingredient, being a cheap and ubiquitous device that integrates many functions required for a colorimetric signal reader. Food control can be performed using reduced resources common at decentralized laboratories. Definitely, this fast DNA biosensing method can support the trending topic of 'Safety from Farm to Fork'.

CRediT authorship contribution statement

Luis A. Tortajada-Genaro: Conceptualization, Investigation, Data curation, Writing – review & editing. **María Isabel Lucío:** Investigation, Writing – review & editing. **Ángel Maquieira:** Supervision.

Declaration of interests

The authors declare that they have no known competing financial interests or personal relationships that could have appeared to influence the work reported in this paper.

Acknowledgments

MINECO Project PID2019-110713RB-I00 and Generalitat Valenciana PROMETEO/2020/094. Students that have supported us during the research.

Appendix A. Supplementary data

Supplementary data to this article can be found online at https://doi.org/10.1016/j.foodcont.2022.108943.

References

Bansal, S., Singh, A., Mangal, M., Mangal, A. K., & Kumar, S. (2017). Food adulteration: Sources, health risks, and detection methods. *Critical Reviews in Food Science and Nutrition, 57*(6), 1174–1189.

Biesiekierski, J. R. (2017). What is gluten? *Journal of Gastroenterology and Hepatology, 32*, 78–81.

Cao, Y. C., Jin, R., & Mirkin, C. A. (2002). Nanoparticles with Raman spectroscopic fingerprints for DNA and RNA detection. *Science, 297*(5586), 1536–1540.

Chang, C. C., Chen, C. P., Wu, T. H., Yang, C. H., Lin, C. W., & Chen, C. Y. (2019). Gold nanoparticle-based colorimetric strategies for chemical and biological sensing applications. *Nanomaterials, 9*(6), 861.

Chen, H., Zhou, K., & Zhao, G. (2018). Gold nanoparticles: From synthesis, properties to their potential application as colorimetric sensors in food safety screening. *Trends in Food Science & Technology, 78*, 83–94.

Deng, H., & Gao, Z. (2015). Bioanalytical applications of isothermal nucleic acid amplification techniques. *Analytica Chimica Acta, 853*, 30–45.

Dincer, C., Bruch, R., Costa-Rama, E., Fernández-Abedul, M. T., Merkoçi, A., Manz, A., … Güder, F. (2019). Disposable sensors in diagnostics, food, and environmental monitoring. *Advanced Materials, 31*(30), 1806739.

García-García, A., Madrid, R., Sohrabi, H., de la Cruz, S., García, T., Martín, R., & González, I. (2019). A sensitive and specific real-time PCR targeting DNA from wheat, barley and rye to track gluten contamination in marketed foods. *LWT, 114*, 108378.

Garrido-Maestu, A., Azinheiro, S., Fuciños, P., Carvalho, J., & Prado, M. (2018). Highly sensitive detection of gluten-containing cereals in food samples by real-time Loop-mediated isothermal AMPlification (qLAMP) and real-time polymerase chain reaction (qPCR). *Food Chemistry, 246*, 156–163.

Giuffrida, M. C., & Spoto, G. (2017). Integration of isothermal amplification methods in microfluidic devices: Recent advances. *Biosensors and Bioelectronics, 90*, 174–186.

González-Domínguez, J. M., León, V., Lucío, M. I., Prato, M., & Vázquez, E. (2018). Production of ready-to-use few-layer graphene in aqueous suspensions. *Nature Protocols, 13*(3), 495–506.

Kanchi, S., Sabela, M. I., Mdluli, P. S., & Bisetty, K. (2018). Smartphone based bioanalytical and diagnosis applications: A review. *Biosensors and Bioelectronics, 102*, 136–149.

Kim, Y. S., Yang, Y., & Henry, C. S. (2018). Laminated and infused Parafilm®–paper for paper-based analytical devices. *Sensors and Actuators B: Chemical, 255*, 3654–3661.

Li, F., Li, F., Yang, G., Aguilar, Z. P., Lai, W., & Xu, H. (2018). Asymmetric polymerase chain assay combined with propidium monoazide treatment and unmodified gold nanoparticles for colorimetric detection of viable emetic Bacillus cereus in milk. *Sensors and Actuators B: Chemical, 255*, 1455–1461.

Li, J., & Macdonald, J. (2015). Advances in isothermal amplification: Novel strategies inspired by biological processes. *Biosensors and Bioelectronics, 64*, 196–211.

Li, H., & Rothberg, L. (2004). Colorimetric detection of DNA sequences based on electrostatic interactions with unmodified gold nanoparticles. *Proceedings of the National Academy of Sciences, 101*(39), 14036–14039.

Lobato, I. M., & O'Sullivan, C. K. (2018). Recombinase polymerase amplification: Basics, applications and recent advances. *TRAC Trends in Analytical Chemistry, 98*, 19–35.

Lo, Y. T., & Shaw, P. C. (2018). DNA-based techniques for authentication of processed food and food supplements. *Food Chemistry, 240*, 767–774.

Santiago-Felipe, S., Tortajada-Genaro, L. A., Puchades, R., & Maquieira, Á. (2016). Parallel solid-phase isothermal amplification and detection of multiple DNA targets in microliter-sized wells of a digital versatile disc. *Microchimica Acta, 183*(3), 1195–1202.

Scherf, K. A., & Poms, R. E. (2016). Recent developments in analytical methods for tracing gluten. *Journal of Cereal Science, 67*, 112–122.

Sharafeldin, M., Kadimisetty, K., Bhalerao, K., Bist, I., Jones, A. L., Chen, T., … Rusling, J. F. (2019). Accessible telemedicine diagnostics with ELISA in a 3D printed pipette tip. *Analytical Chemistry, 91*, 7394–7402.

Srimongkol, G., Ditmangklo, B., Choopara, I., Thaniyavarn, J., Dean, D., Kokpol, S., … Somboonna, N. (2020). Rapid colorimetric loop-mediated isothermal amplification for hypersensitive point-of-care Staphylococcus aureus enterotoxin A gene detection in milk and pork products. *Scientific Reports, 10*(1), 1–11.

Tortajada-Genaro, L. A., Yamanaka, E. S., & Maquieira, Á. (2019). Consumer electronics devices for DNA genotyping based on loop-mediated isothermal amplification and array hybridisation. *Talanta, 198*, 424–431.

Valentini, P., & Pompa, P. P. (2013). Gold nanoparticles for naked-eye DNA detection: Smart designs for sensitive assays. *RSC Advances, 3*(42), 19181–19190.

Valentini, P., & Pompa, P. P. (2016). A universal polymerase chain reaction developer. *Angewandte Chemie International Edition, 55*(6), 2157–2160.

Yamanaka, E. S., Tortajada-Genaro, L. A., Pastor, N., & Maquieira, Á. (2018). Polymorphism genotyping based on loop-mediated isothermal amplification and smartphone detection. *Biosensors and Bioelectronics, 109*, 177–183.

Yang, K., Peretz-Soroka, H., Liu, Y., & Lin, F. (2016). Novel developments in mobile sensing based on the integration of microfluidic devices and smartphones. *Lab on a Chip, 16*(6), 943–958.

Ye, X., Fang, X., Li, X., & Kong, J. (2018). Gold nanoparticle-mediated nucleic acid isothermal amplification with enhanced specificity. *Analytica Chimica Acta, 1043*, 150–157.

Yun, W., Jiang, J., Cai, D., Zhao, P., Liao, J., & Sang, G. (2016). Ultrasensitive visual detection of DNA with tunable dynamic range by using unmodified gold nanoparticles and target catalyzed hairpin assembly amplification. *Biosensors and Bioelectronics, 77*, 421–427.

Yu, L., & Shi, Z. Z. (2015). Microfluidic paper-based analytical devices fabricated by low-cost photolithography and embossing of Parafilm. *Lab on a Chip, 15*(7), 1642–1645.

Yu, T., & Wei, Q. (2018). Plasmonic molecular assays: Recent advances and applications for mobile health. *Nano Research, 11*(10), 5439–5473.

Zhao, Y., Chen, F., Li, Q., Wang, L., & Fan, C. (2015). Isothermal amplification of nucleic acids. *Chemical Reviews, 115*(22), 12491–12545.

Zou, L., Shen, R., Ling, L., & Li, G. (2018). Sensitive DNA detection by polymerase chain reaction with gold nanoparticles. *Analytica Chimica Acta, 1038*, 105–111.